Zeitschrift für Kristallographie

International journal for structural, physical, and chemical aspects of crystalline materials

R. Oldenbourg Verlag
München

Disorder of Cu⁺ in Cu₃SbS₃: structural investigations of the high- and low-temperature modification

$\text{Disorder of } Cu^+ \text{ in } Cu_3SbS_3$

A. Pfitzner*

Universität-Gesamthochschule Siegen, Anorganische Chemie, D-57068 Siegen, Germany

Abstract. The crystal structure of α-Cu_3SbS_3 at 493 K and 403 K was determined from single crystal data. The high-temperature modification, which is stable above 394 K, crystallizes in the orthorhombic system, space group $Pnma$ (No. 62), $a = 7.808(1)$ Å, $b = 10.252(2)$ Å, $c = 6.587(2)$ Å, and $Z = 4$ ($T = 493$ K). From single crystal data the distribution of the disordered copper atoms in the three-dimensional arrangement of $[SbS_3]^{3-}$ units was determined. The atomic displacement parameters of the disordered copper atoms were refined using a Gram-Charlier non-harmonic development and a suggestion for a pathway for mobile copper atoms is derived. Copper atoms are distributed over five sites with trigonal planar or tetrahedral coordination and empty octahedra S_6 are the bottlenecks for a three-dimensional movement. The crystal structure of γ-Cu_3SbS_3, which is stable below 264 K, was determined from X-ray powder data by the Rietveld method. The low-temperature modification crystallizes also in the orthorhombic system, space group $P2_12_12_1$ (No. 19), $a = 7.884(1)$ Å, $b = 10.221(1)$ Å, $c = 6.624(1)$ Å, and $Z = 4$ ($T = 223$ K). Whereas the arrangement of the thioantimonate(III) polyhedra keeps almost unchanged the copper atoms in the low-temperature modification γ-Cu_3SbS_3 are no longer disordered but are located in three different positions with triangular coordination by sulfur.

Introduction

Cu_3SbS_3, which is known as the mineral skinnerite [1], is a member of the group of the so-called sulfosalts. Thus it belongs to a group of ca. 130 [2] naturally occurring chalcogenides (mainly sulfides), which all have in common a trigonal pyramidally coordinated As^{3+}, Sb^{3+}, Bi^{3+} or Te^{4+} cation in their structures. They attract scientific interest not only as ores but also as promising materials for applications in photovoltaic systems [3]. Nevertheless the crystal chemistry of Cu_3SbS_3, especially of the high- and low-temperature modification, is still not fully clear. Despite

the fact that this compound has been investigated by several authors, structural data of the β-modification, which is stable at room temperature, have been published recently [4, 5]. The crystal structures of the low-temperature modification γ and the high-temperature modification α have not yet been determined in detail but a discussion of possible ordering schemes for copper atoms in a matrix of trigonal thioantimonate(III) pyramids was given by Makovicky [6]. In accordance with Whitfield [7] he suggested the Cu_3BiS_3-type [8, 9] as one of the possible structures for γ-Cu_3SbS_3.

The phase transformations between the different polymorphs and problems related to these transformations (twinning, crystal disintegration, copper disorder, etc.) might be regarded as reasons that reliable structural data are still lacking for the high- and low-temperature polymorph. Thus the structures of the α-modification, which is supposed to show high copper ion conductivity or at least a high copper diffusion coefficient [1, 10–13], and of the γ-polymorph are presented here. Also the relationships between the three modifications of Cu_3SbS_3 and Cu_3SbSe_3, which shows an alternative ordering scheme of copper in an almost unchanged chalcogenoantimonate(III) sublattice and a tetrahedral coordination for all copper atoms [14], are discussed.

Experimental

Cu_3SbS_3 has been prepared by the reaction of Cu_2S and Sb_2S_3 at 853 K in evacuated quartz ampoules, for details see [4]. The high-temperature data were obtained from the same single crystal, which was used earlier for the structure determination of the room temperature modification β-Cu_3SbS_3. Precession photographs of α-Cu_3SbS_3, which is stable above 394 K, were obtained using a home made hot gas-blowing device, and intensity data were collected on a Nonius CAD4 (Nonius heating goniometer head). JANA96 [15] was used for the structure refinements including a non-harmonic expansion of the copper atomic displacement parameters, Fourier syntheses and contour plots.

For γ-Cu_3SbS_3, which is stable below 264 K [4, 7], no single crystal data could be obtained. Several attempts

* e-mail: pfitzner@chemie.uni-siegen.de

to collect data of the low-temperature modification failed because the single crystals always disintegrated during the first order phase transition from the β- to the γ-modification. Thus powder data at 223 K were collected on a Siemens D5000 using monochromatized $CuK_{\alpha 1}$ radiation in transmission setup and a home made cold nitrogen gas-blowing device. Rietveld refinements were performed with the FULLPROF program package [16], using the atomic parameters of Cu_3BiS_3 [8, 9] as starting values. Structural data of $Cu_{12}Sb_4S_{13}$, which was observed as an impurity in the powder pattern, were included in the powder refinement. Keeping the measurement temperature of 223 K in mind the lattice constant of $a = 10.317(1)$ Å indicates that this phase has to be assigned to the low copper end member of the $Cu_{12+x}Sb_4S_{13}$ series [17, 18].

Results

α-Cu₃SbS₃

Crystallographic data for α-Cu₃SbS₃ at 403 K and 493 K are collected in Table 1, the refinement results are given in Tables 2–4. Using only anisotropic (harmonic) atomic displacement parameters for the copper atoms, the refinements converged at $R = 0.0399$ (67 parameters, 804 reflections, $T = 403$ K), and $R = 0.0457$ (67 parameters, 808 reflections, $T = 493$ K), respectively. Especially the displacement parameters in this model, e.g. $U^{22}(Cu(5)) =$

0.9(2) Å² ($T = 493$ K), were not satisfactory. Thus nonharmonic displacement parameters up to fourth order for the copper atoms Cu(1)−Cu(3) were introduced in the refinement. In order to get a sufficient number of reflections per refined parameter all reflections were used for the refinement despite the fact that the R-values became slightly higher. Additionally, only those non-harmonic tensor elements, which were above a three-σ level, were considered in the final refinement cycles, the rest of them was regarded as not significant and thus fixed to zero [19]. By this addition of a limited number of parameters the quality of the models was improved as indicated by $R = 0.0345$ (84 parameters, 804 reflections, $T = 403$ K), and $R = 0.0357$ (89 parameters, 808 reflections, $T = 493$ K). The significance of the model was checked by statistical tests [20]. For $T = 403$ K one finds R(harmonic)/R(non-harmonic) = 1.157, and for 493 K the corresponding ratio takes a value of 1.280. Both data are far above the necessary limits which are 1.025 ($T = 403$ K) and 1.030 ($T = 493$ K). In addition the probability density function (p.d.f.) sections show no significant negative regions and thus the non-harmonic models can be regarded as valid [21].

Selected interatomic distances and angles are summarized in Table 5. The differences between the refined positions of the copper atoms Cu(1)−Cu(3) and the positions of the maxima in the p.d.f. (mode positions) are <0.2 Å, and the mode positions have been used for distance calculations.

Table 1. Crystallographic data (e.s.d.s) for the structure determinations of α-Cu₃SbS₃[a].

Compound/modification	α-Cu₃SbS₃	
Formula weight (g mol⁻¹)	408.568	
Crystal size (mm³)	0.15 × 0.2 × 0.2	
Crystal system	orthorhombic	
Space group	$Pnma$ (No. 62)	
Measuring temperature (K)	403	493
Lattice constants (Å)	$a = 7.802(2)$	7.808(1)
(single crystal data)	$b = 10.238(4)$	10.252(2)
	$c = 6.595(3)$	6.587(2)
d_x (g cm⁻³)	5.152	5.147
Lin. absorption coefficient μ_{MoK_α} (cm⁻¹)	180.95	180.78
Diffractometer	CAD4, MoK_α (0.71073 Å), graphite monochromator, scintillation counter, Nonius heating device	
Scan type	ω-scan	
Absorption correction	ψ-scans	
2θ-range (°)	$0° < 2\theta \leq 60°$	
Data range	$0 \leq h \leq 10$	
	$0 \leq k \leq 14$	
	$0 \leq l \leq 9$	
Number of reflections	804	808
Number of reflections used	804	808
Number of reflections with $I > 2\sigma(I)$	735	754
Refined parameters	84	89
R (all reflections)	0.0345	0.0357
wR (all reflections)	0.0767	0.0858
g.o.f.	2.58	3.18
Extinction coefficient	0.19(2)	0.25(2)
Residual electron density		
$\Delta\varrho_{min}/\Delta\varrho_{max}$ (e Å⁻³)	−1.00 / 1.03	−0.80 / 1.68
Refinement	JANA96 [15], full matrix least squares based on F^2	

a: Additional material to this paper can be ordered referring to the no. CSD 403111 (403 K) and CSD 403112 (493 K), name of the author and citation of the paper at the Fachinformationszentrum Karlsruhe, Gesellschaft für wissenschaftlich-technische Information mbH, D-76344 Eggenstein-Leopoldshafen, Germany. The list of F_o/F_c-data is available from the author up to one year after the publication has appeared.

Table 2. Atomic parameters (e.s.d.s) and U_{eq}[a] (Å^2) of α-Cu$_3$SbS$_3$ at 403 K and 493 K.

Atom	Site	x	y	z	s.o.f.	U_{eq}
T = 403 K						
Sb	4c	0.27564(5)	$^1/_4$	0.88324(7)	1.	0.0331(1)
S(1)	4c	0.0485(2)	$^1/_4$	0.1428(2)	1.	0.0383(4)
S(2)	8d	0.1715(1)	0.06863(10)	0.6724(2)	1.	0.0325(3)
Cu(1)	8d	0.0699(2)	0.0329(2)	0.2171(4)	0.486(4)	0.0563(6)
Cu(2)	8d	0.3476(8)	0.1012(7)	0.4084(4)	0.400(6)	0.069(2)
Cu(3)	8d	0.1865(14)	0.0954(3)	0.3360(5)	0.530(8)	0.147(4)
Cu(4)	4c	0.0800(16)	$^1/_4$	0.456(2)	0.074(4)	0.046(4)
Cu(5)	4c	0.229(4)	$^1/_4$	0.425(4)	0.050(6)	0.08(1)
T = 493 K						
Sb	4c	0.27349(5)	$^1/_4$	0.88343(6)	1.	0.0361(2)
S(1)	4c	0.0453(2)	$^1/_4$	0.1418(2)	1.	0.0421(5)
S(2)	8d	0.1706(1)	0.06852(10)	0.6718(2)	1.	0.0351(4)
Cu(1)	8d	0.0723(3)	0.0337(2)	0.2169(5)	0.480(6)	0.069(2)
Cu(2)	8d	0.3428(11)	0.1041(10)	0.4077(6)	0.382(7)	0.089(2)
Cu(3)	8d	0.1776(15)	0.0913(5)	0.3323(6)	0.518(9)	0.167(6)
Cu(4)	4c	0.0805(16)	$^1/_4$	0.4585(15)	0.080(4)	0.048(4)
Cu(5)	4c	0.227(3)	$^1/_4$	0.430(3)	0.082(8)	0.09(1)

a: U_{eq} is defined as one third of the trace of the orthogonalized U^{ij} tensor.

Table 3. Anisotropic displacement parameters U^{ij} (Å^2) for α-Cu$_3$SbS$_3$ at 403 K and 493 K.

Atom	U^{11}	U^{22}	U^{33}	U^{13}	U^{12}	U^{23}
T = 403 K						
Sb	0.0298(2)	0.0262(2)	0.0432(3)	0	−0.0031(1)	0
S(1)	0.0508(9)	0.0244(6)	0.0397(8)	0	0.0088(6)	0
S(2)	0.0374(5)	0.0251(4)	0.0351(5)	0.0005(4)	0.0003(4)	−0.0003(4)
Cu(1)	0.0421(7)	0.0400(8)	0.087(2)	0.0020(5)	0.0050(8)	0.0098(8)
Cu(2)	0.077(2)	0.083(4)	0.048(1)	−0.048(3)	0.0042(9)	−0.0023(9)
Cu(3)	0.29(1)	0.105(4)	0.052(1)	0.119(4)	0.053(3)	0.026(1)
Cu(4)	0.047(8)	0.049(7)	0.043(7)	0	−0.004(5)	0
Cu(5)	0.08(2)	0.10(3)	0.05(1)	0	0.00(1)	0
T = 493 K						
Sb	0.0329(3)	0.0293(3)	0.0462(3)	0	−0.0040(1)	0
S(1)	0.0585(10)	0.0270(7)	0.0407(7)	0	0.0091(6)	0
S(2)	0.0423(5)	0.0275(5)	0.0356(5)	0.0007(4)	−0.0003(4)	−0.0003(3)
Cu(1)	0.0483(9)	0.0467(10)	0.113(5)	0.0040(6)	0.0091(9)	0.0133(10)
Cu(2)	0.010(4)	0.111(5)	0.057(1)	−0.066(3)	0.011(1)	−0.005(1)
Cu(3)	0.30(1)	0.139(6)	0.061(2)	0.145(6)	0.061(4)	0.040(2)
Cu(4)	0.056(8)	0.053(7)	0.034(5)	0	−0.001(4)	0
Cu(5)	0.12(2)	0.10(2)	0.049(8)	0	−0.003(8)	0

Table 4. Non-harmonic displacement parameters[a] for the copper atoms.

	T = 403 K			*T* = 493 K		
	Cu(1)	Cu(2)	Cu(3)	Cu(1)	Cu(2)	Cu(3)
C_{111}		−0.23(4)	0.5(1)		−0.51(7)	0.41(9)
C_{112}	0.020(5)	0.21(3)		0.036(5)	0.45(5)	
C_{113}			0.28(5)		−0.10(2)	0.24(4)
C_{122}		−0.20(3)			−0.46(5)	
C_{133}	0.12(1)		0.10(3)	0.18(2)		0.10(3)
C_{222}		0.15(3)			0.41(6)	
C_{223}		0.054(8)			0.06(1)	
D_{1111}			−3(1)			−25(2)
D_{1112}		−0.7(1)			−1.0(2)	−6.1(7)
D_{1113}						−2.4(4)
D_{1122}		0.8(1)			1.4(3)	−1.4(3)
D_{1222}		−0.9(2)			−1.6(3)	
D_{1223}	−0.09(3)			−0.14(3)		
D_{2222}		0.9(2)	0.3(1)		1.7(3)	0.7(2)
D_{3333}			5(1)			

a: Third-order elements C_{pqr} are multiplied by 10^4, fourth-order elements D_{pqrs} are multiplied by 10^6.

The displacement parameters are defined as:

$$T_{GC}(\bar{h}) = T_{harm}(\bar{h})\left[1 + \frac{(2\pi i)^3}{3!}C_{pqr}h_p h_q h_r + \frac{(2\pi i)^4}{4!}D_{pqrs}h_p h_q h_r h_s\right]$$

Table 5. Selected interatomic distances (Å) and angles (°) for α- and γ-Cu₃SbS₃ᵃ.

α-Cu₃SbS₃ (493 K)

Sb	−S(1)	2.464(2)	S(1)−Sb−S(2) 2x	98.92(4)
	−S(2) 2x	2.460(1)	S(2)−Sb−S(2)	98.30(4)
	−Cu(4)	2.61(1)	S(1)−Sb−Cu(4)	112.8(2)
			S(2)−Sb−Cu(4) 2x	121.7(1)
Cu(1)*	−S(1)	2.300(2)	S(1)−Cu(1)*−S(2)	116.4(1)
	−S(2)	2.260(3)	S(1)−Cu(1)*−S(2)'	118.7(1)
	−S(2)'	2.295(3)	S(2)−Cu(1)*−S(2)'	124.9(1)
Cu(2)*	−S(1)	2.171(10)	S(1)−Cu(2)*−S(2)	129.4(4)
	−S(2)	2.294(7)	S(1)−Cu(2)*−S(2)'	119.8(3)
	−S(2)'	2.308(8)	S(2)−Cu(2)*−S(2)'	110.9(4)
Cu(3)*	−S(1)	2.244(6)	S(1)−Cu(3)*−S(2)	128.2(3)
	−S(2)	2.286(4)	S(1)−Cu(3)*−S(2)'	119.9(2)
	−S(2)'	2.323(8)	S(2)−Cu(3)*−S(2)'	110.6(3)
Cu(4)	−S(1)	2.105(10)	S(1)−Cu(4)−S(2) 2x	127.6(2)
	−S(2) 2x	2.435(7)	S(2)−Cu(4)−S(2)'	99.6(4)
	−Sb	2.61(1)	S(1)−Cu(4)−Sb	106.0(5)
			S(2)−Cu(4)−Sb 2x	92.0(3)
Cu(5)	−S(1)	2.37(2)	S(1)−Cu(5)−S(1)	116.1(8)
	−S(1)'	2.53(3)	S(1)−Cu(5)−S(2) 2x	114.0(8)
	−S(2) 2x	2.49(1)	S(2)−Cu(5)−S(2)'	96.7(7)

γ-Cu₃SbS₃ (223 K)

Sb	−S(1)	2.45(2)	S(1)−Sb−S(2)	99.5(6)
	−S(2)	2.45(3)	S(1)−Sb−S(3)	96.1(6)
	−S(3)	2.50(3)	S(2)−Sb−S(3)	97.5(6)
Cu(1)	−S(1)	2.20(2)	S(1)−Cu(1)−S(3)	125.8(7)
	−S(3)	2.33(2)	S(1)−Cu(1)−S(3)'	121.5(7)
	−S(3)'	2.31(2)	S(3)−Cu(1)−S(3)'	111.1(7)
Cu(2)	−S(1)	2.27(2)	S(1)−Cu(2)−S(2)	133.2(7)
	−S(2)	2.25(2)	S(1)−Cu(2)−S(2)'	115.6(7)
	−S(2)'	2.32(2)	S(2)−Cu(2)−S(2)'	110.4(7)
Cu(3)	−S(1)	2.35(2)	S(1)−Cu(3)−S(2)	116.9(7)
	−S(2)	2.28(2)	S(1)−Cu(3)−S(3)	114.2(7)
	−S(3)	2.36(2)	S(2)−Cu(3)−S(3)	128.3(8)

a: Atoms marked with a star superscript refer to the mode positions which are Cu(1)* [0.0697(3), 0.0319(2), 0.2180(5)], Cu(2)* [0.358(1), 0.097(1), 0.4076(6)], and Cu(3)* [0.156(2), 0.0866(5), 0.3262(6)].

γ-Cu₃SbS₃

In Table 6 crystallographic and experimental data for the structure determination of the low-temperature polymorph γ-Cu₃SbS₃ are collected. Table 7 contains the refined

Table 6. Data collection and refinement parameters for γ-Cu₃SbS₃ at 223 Kᵃ.

Diffractometer	Siemens D5000, CuKα1, λ = 1.54051 Å, Braun linear PSD, active range = 1 cm
2θ-range (°)	15−80
Stepwidth (°), time per step (s)	0.015378, 9
Zero point (°)	0.039(1)
No. of background points	24
Space group	P2₁2₁2₁ (No. 19)
Lattice constants (Å)	a = 7.884(1), b = 10.221(1), c = 6.624(1)
Volume (Å³), Z	533.7(1), 4
M (g mol⁻¹)	408.568
dₓ (g cm⁻³)	5.083
No. of reflections	212
No. of refined parameters	44
Profile function	Pearson VII
M (Pearson VII exponent)	1.20(1)
Halfwidth parameters (°²)	U = 0.059(4), V = −0.034(3), W = 0.0128(7)
Asymmetry parameters	P1 = 0.103(6), P2 = 0.028(1)
Agreement factors	Rₚ = 0.0376, Rwp = 0.0495
Refinement program	Fullprof 3.1c [16]

a: Additional materials to this paper can be ordered referring to the no. CSD 403113 (223 K), name of the author and citation of the paper at the Fachinformationszentrum Karlsruhe, Gesellschaft für wissenschaftlich-technische Information mbH, D-76344 Eggenstein-Leopoldshafen, Germany. The list of F₀/Fc-data is available from the author up to one year after the publication has appeared.

Table 7. Atomic parameters (e.s.d.s)ᵃ and Bᵢₛₒ (Å²) of γ-Cu₃SbS₃ at 223 Kᵃ.

Atom	Site	x	y	z	Bᵢₛₒ
Sb	4a	0.2793(4)	0.2462(7)	0.6280(6)	1.9(1)
S(1)	4a	0.050(2)	0.250(2)	0.878(2)	0.9(2)
S(2)	4a	0.180(2)	0.066(2)	0.414(2)	0.9(2)
S(3)	4a	0.169(2)	0.430(2)	0.417(2)	0.9(2)
Cu(1)	4a	0.3464(11)	0.3967(9)	0.1413(15)	3.0(3)
Cu(2)	4a	0.1835(11)	0.1031(9)	0.0800(14)	3.0(2)
Cu(3)	4a	0.0661(11)	0.4700(9)	0.9805(14)	2.1(2)

a: The e.s.d.s obtained after the last refinement cycle were multiplied by a factor of 2.05 [27].

atomic parameters and isotropic displacement parameters. The Bᵢₛₒ values for the three independent sulfur atoms in γ-Cu₃SbS₃ were constrained whereas those of the heavier atoms antimony and copper were refined independently. The quality of the refinement can be judged either from the agreement factors (see Table 6) or from the graphical presentation of the measured and calculated diffraction pattern which is shown in Fig. 1.

Discussion

General structural features

In the crystal structures of Cu₃SbQ₃ (Q = S, Se) trigonal pyramidal trichalcogenoantimonate(III) units [SbQ₃]³⁻ provide a three-dimensional network, which contains numerous favorable sites for the location of copper. Occupation of these positions results in either trigonal planar or tetrahedral coordination for the copper atoms. Taking distance limitations between the copper atoms and symmetry restrictions into consideration different crystal structures result if copper atoms are located on the possible positions (note that not all of them can be occupied at the same time in ordered structures). According to Hyde and Andersson [22] the crystal structure of Cu₃SbS₃ (without respect to the actual modification) can be derived from the
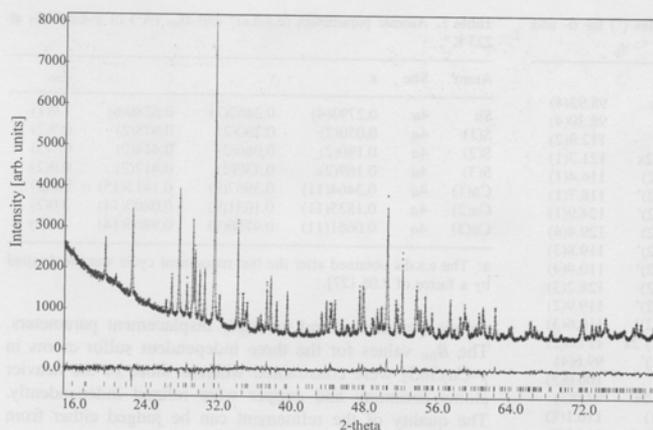
Fig. 1. Observed, calculated and difference X-ray powder diffraction pattern for γ-Cu$_3$SbS$_3$ at 223 K. Calculated reflection positions of γ-Cu$_3$SbS$_3$ and of the impurity Cu$_{12}$Sb$_4$S$_{13}$ are marked by vertical bars.

cementite-type (Fe$_3$C) in the way that sulfur replaces iron atoms. Thus sheets of octahedra S$_6$ and trigonal prisms S$_6$ alternate along [010], see Fig. 2. Antimony is located near the carbon site in the trigonal prisms. Additionally, tetrahedral and tetragonal-pyramidal voids result, and face sharing of tetrahedra results in the formation of trigonal-bipyramids.

In the following the relations between the crystal structures of the three modifications of Cu$_3$SbS$_3$ and of Cu$_3$SbSe$_3$, respectively, are described in a schematic way. As shown in Fig. 3 the arrangement of the chalcogenoantimonate(III) ions in these compounds remains more or less the same but copper is distributed over different sites, depending on the temperature and the type of the chalcogenide ion. The three modifications of Cu$_3$SbS$_3$ and Cu$_3$SbSe$_3$ all have in common that the octahedra Q$_6$ are empty and
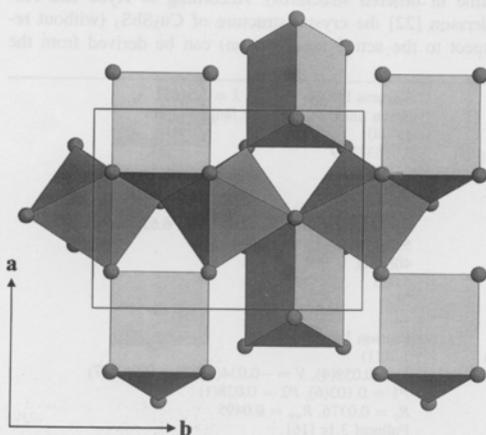

Fig. 2. Section of the crystal structure of Cu$_3$SbQ$_3$ (Q = S, Se) emphasizing the analogy to the Fe$_3$C-type. The octahedra Q$_6$ are empty in Cu$_3$SbQ$_3$, and antimony is located off-center in the trigonal prisms. Note that only a small section is drawn in order to show the sequence of octahedra and trigonal prisms along [010].

copper is located on two of their eight triangular faces. In case of α-Cu$_3$SbS$_3$ even four faces are — only partly — occupied by copper. Thus for all compounds under discussion two of three copper atoms per formula unit are distributed on the octahedron's faces (taking into account the site occupancy factors in α-Cu$_3$SbS$_3$, see Table 2). The rest of them is located between the octahedra Q$_6$ and has either trigonal planar coordination (α-Cu$_3$SbS$_3$, β-Cu$_3$SbS$_3$, γ-Cu$_3$SbS$_3$) or tetrahedral coordination (α-Cu$_3$SbS$_3$, Cu$_3$SbSe$_3$). In case of (CuI)$_2$Cu$_3$SbS$_3$, which can be regarded as a solid solution of Cu$_3$SbS$_3$ in CuI, even six faces of similar octahedra S$_6$ are partly occupied by Cu [23].

In Fig. 4a–c the three different possibilities, how two faces of an octahedron can be centered by copper atoms, are shown. One way is the centering of two opposite faces (type 1), the second one is the centering of two faces sharing a common vertex (type 2), and the third one is the centering of two faces with a common edge (type 3). Due to distance limitations between the copper atoms type 3 can only be observed in disordered structures and only one of the two positions of a given octahedron can be occupied at the same time.

The principal building scheme of the crystal structures of the Cu$_3$SbS$_3$ polymorphs and of Cu$_3$SbSe$_3$ can be rationalized by combination of these different octahedron types. Thus in the low-temperature modification γ-Cu$_3$SbS$_3$ all octahedra are of type 2. By contrast in the room temperature modification β-Cu$_3$SbS$_3$ octahedra of type 1 and type 2 are observed. They are arranged in a way, that alternating sheets of octahedra parallel (100) are either of type 1 or of type 2. A doubled *c*-axis with respect to the small orthorhombic cell *a*, *b*, *c* results. In the high-temperature polymorph α-Cu$_3$SbS$_3$ four faces of the octahedra are statistically occupied, see Fig. 4d (type 4). The positions of Cu(1) and Cu(2) are arranged in type 3, but since the distance between these sites is too small (d(Cu(1)–Cu(2)) < 2.1 Å) only one of them can be occupied at the same time. Thus the arrangement of type 3 is only pretended as an average over time and space by the X-ray structure determination. Both, type 1 for the pair
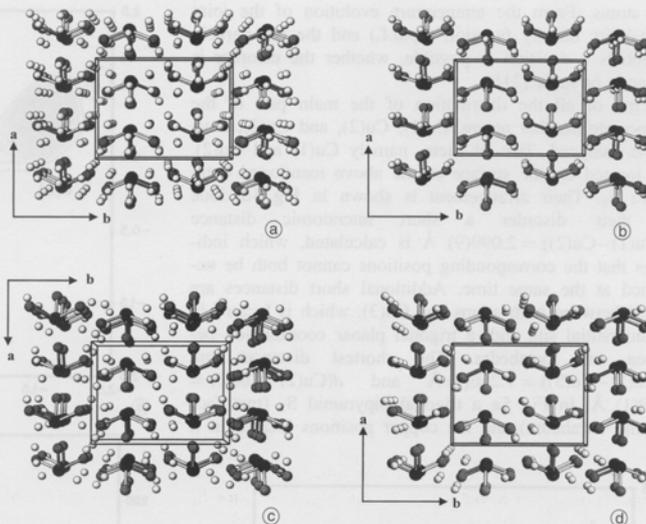
Fig. 3. Sections of the crystal structures of **a)** α-Cu₃SbS₃, **b)** Cu₃SbSe₃, **c)** β-Cu₃SbS₃, and **d)** γ-Cu₃SbS₃. Antimony: large dark spheres, sulfur/selenium: gray spheres, and copper: small white spheres. Bonds between copper and chalcogen atoms are omitted for clarity. Note that for α-Cu₃SbS₃ the copper positions are not fully occupied. Data for **b)** and **c)** are taken from refs. [4, 14]. The doubled c axis of β-Cu₃SbS₃ becomes not fully visible in this representation.
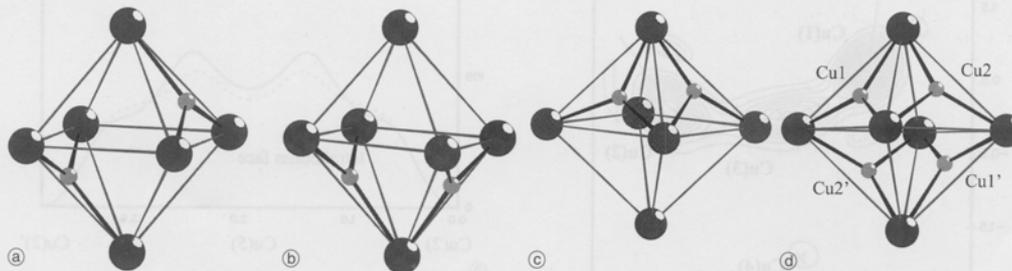
Fig. 4. Possible ways how two copper atoms can center the faces of an octahedron Q_6. **a)** Type 1, two opposite faces, **b)** type 2, two faces sharing one corner, and **c)** type 3, two faces with a common edge. Note that type 3 results in an unreasonable short distance between the corresponding copper atoms, this type can only be observed in disordered structures. **d)** Addition of a center of symmetry to the octahedron of type 3 provides the distribution of copper atoms in the disordered high-temperature phase α-Cu₃SbS₃.

Cu(1)−Cu(1)' and type 2 for e.g. the combination Cu(1)-Cu(2)' are possible at the same time with respect to the interatomic distances. The fourth three-dimensional distribution of octahedra is found in the crystal structure of Cu₃SbSe₃. All octahedra are of type 1, which is only possible since the third copper atom is shifted towards a tetrahedrally coordinated position in the sheets of trigonal prisms, cf. [14].

Copper disorder in the high-temperature modification α-Cu₃SbS₃

In order to clear up the nature of the copper disorder in the high-temperature modification of Cu₃SbS₃ X-ray datasets were collected at 403 K and 493 K and the crystal structure was refined with a Gram-Charlier non-harmonic development for the displacement parameters of the cop-

Fig. 5. Section of the crystal structure of α-Cu₃SbS₃ showing the trigonal pyramidal arrangement of sulfur atoms around Cu(3) and the positions of Cu(1) and Cu(2) **a)** in a ball and stick representation and **b)** showing a 3D surface of the j.p.d.f. for Cu(1), Cu(2), and Cu(3). Note the deformation of Cu(2) towards the front face of the coordinating tetrahedron.
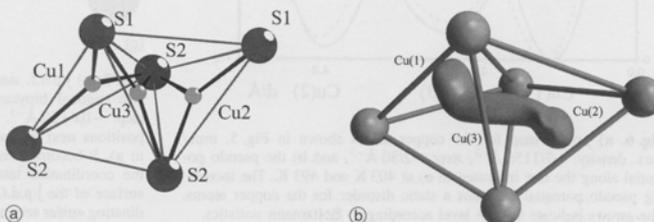
per atoms. From the temperature evolution of the joint probability density function (j.p.d.f.) and the one-particle potentials a decision is possible, whether the disorder is dynamic or static [21].

First of all the distribution of the main part of the copper atoms, that means Cu(1), Cu(2), and Cu(3), have to be analyzed. Two of them, namely Cu(1) and Cu(2), are located on the surface of the above mentioned octahedra S_6. Their arrangement is shown in Fig. 4d. Due to their disorder a short interatomic distance $d(Cu(1)-Cu(2)) = 2.099(9)$ Å is calculated, which indicates that the corresponding positions cannot both be occupied at the same time. Additional short distances are found between both atoms and Cu(3), which is located in an interstitial site with a trigonal planar coordination between two octahedra. The shortest distances are $d(Cu(1)-Cu(3)) = 1.266(9)$ Å and $d(Cu(2)-Cu(3)) = 1.39(1)$ Å. In Fig. 5a a trigonal bipyramid S_5 (two face sharing tetrahedra) and the copper positions located in it
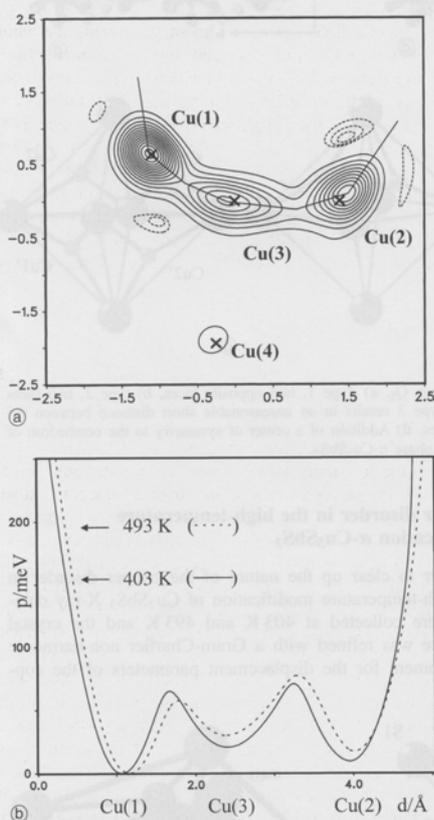
Fig. 6. **a)** j.p.d.f. map for the copper atoms shown in Fig. 5, min./max. density: $-7/1156$ Å^{-3}, step: $-2/80$ Å^{-3}, and **b)** the pseudo potential along the line indicated in **a)** at 403 K and 493 K. The increasing pseudo potential indicates a static disorder for the copper atoms. The arrows indicate the 1% level according to Boltzmann statistics.
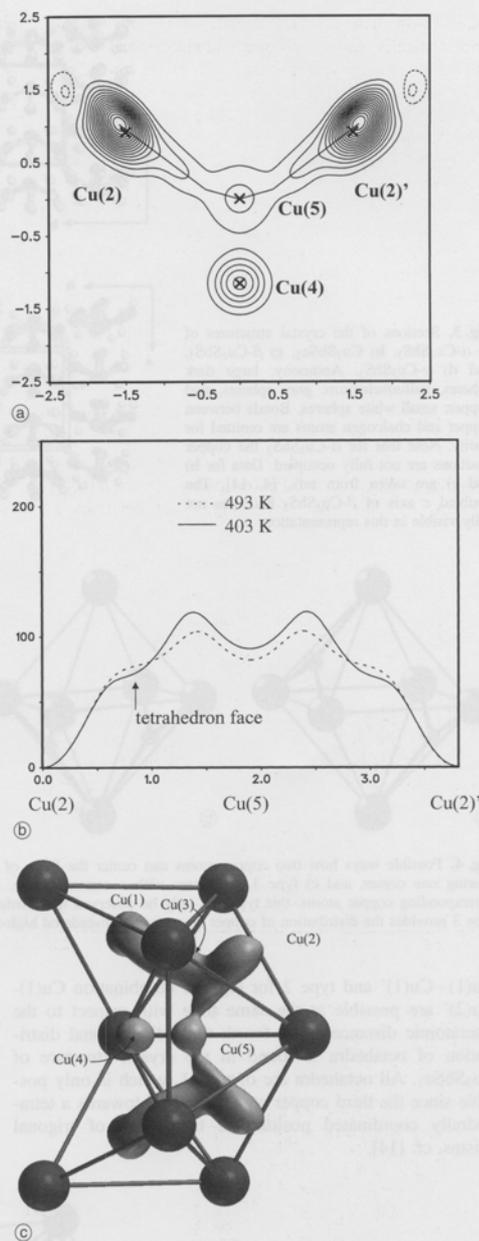
Fig. 7. **a)** j.p.d.f. map around Cu(5), which acts as a bridge between two trigonal bipyramids S_5 (cf. Fig. 5b), min/max: $-22/796$ Å^{-3}, step: $-10/+50$ Å^{-3}. The plane is defined by [010] and the two Cu(2) positions next to Cu(5). **b)** Pseudo potential along the line indicated in **a)**. It becomes visible that the common face of the bipyramid and the coordination tetrahedron around Cu(5) is also occupied. **c)** 3D surface of the j.p.d.f. for the copper atoms around Cu(5) in the coordinating sulfur tetrahedra.

are shown. The distance $d(Cu(1)-Cu(2)) = 2.566(7)$ Å is not critically short for copper chalcogenides. This means that in a trigonal bipyramid S_5 either the Cu(1)- and Cu(2)-site or the Cu(3)-site can be occupied at the same time. In Fig. 6 a j.p.d.f. map and the potential curves at 403 K and 493 K are shown for these three copper atoms. Since the single p.d.f.s are strongly overlapping the derived potential curve is only a pseudo potential, the real potential between the different sites is higher. This already becomes visible from its temperature evolution. The potential maxima calculated at 493 K are higher than those at 403 K. According to [21] this behavior is an indication for a static disorder. Nevertheless one can assume that the copper atoms are readily distributed over all of these sites. A 3D surface plot of the j.p.d.f. of Cu(1), Cu(2), and Cu(3) in the trigonal bipyramid S_5 is shown in Fig. 5 b.

Two of these bipyramidal coordination spheres for copper (cf. Fig. 5) share faces with a tetrahedral void in which Cu(5) is located. The corresponding j.p.d.f. map is shown in Fig. 7a, the derived pseudo potential in Fig. 7b. From the 3D surface plot (Fig. 7c) it becomes obvious,
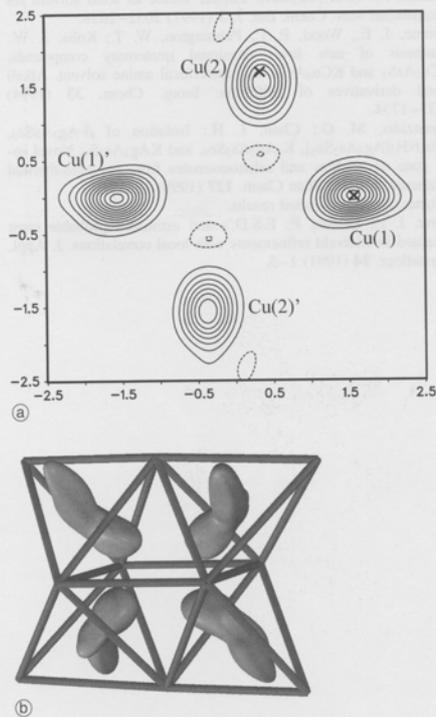
Fig. 8. a) j.p.d.f. map at 493 K for the copper atoms around the octahedral voids in α-Cu_3SbS_3, min/max: $-10/1146$ Å^{-3}, step: $-5/100$ Å^{-3}. The plane is defined by the origin, Cu(1) and Cu(2). The potential connecting the different maxima in the p.d.f. (not shown) is much higher than the 1% cut-off according to Boltzmann statistics. **b)** 3D surface of the j.p.d.f. for the copper atoms on the octahedron's faces and the face sharing tetrahedra.

that the interstitial position of Cu(5) is a bridge between the copper atoms in two mirror related trigonal bipyramids. A significant occupation of the face which connects the central tetrahedron and the bipyramids is also shown. Cu(4) is located in a trigonal prism together with Sb. From geometrical considerations one can assume that Cu(4) coordinates to the lone pair of a Sb^{3+} ion. Thus a relatively short distance $d(Sb-Cu(4)) = 2.61(1)$ Å (493 K) results. Only a few compounds are known, where the lone-pair of an As^{3+} or Sb^{3+} cation is coordinated by Cu^+ or Ag^+. In KCu_2AsS_3, for example, arsenic ions are tetrahedrally coordinated by one copper and three sulfur atoms with $d(As^{3+}-Cu) = 2.61$ Å [24]. In $(Me_3NH)[Ag_3As_2Se_5]$ a distance $d(As^{3+}-Ag) = 2.844$ Å was found [25]. In sulfur rich compounds of the series $Cu_3SbS_{3-x}Se_x$ a threefold superstructure of the Cu_3SbQ_3 type is due to exactly the same $Sb^{3+}-Cu^+$ pairs observed in α-Cu_3SbS_3, but in the mixed sulfide selenide these pairs are formed only for every third antimony atom and the corresponding copper position is fully occupied [26].

Up to now no three-dimensional pathway for copper atoms in α-Cu_3SbS_3 has been shown. Analyzing the whole structure with respect to this point reveals the octahedra S_6 to be the bottlenecks for a connection of the areas where copper is locally disordered. Each octahedron shares common faces with four trigonal bibyramids of the above mentioned type, but as already described there is no electron density found inside of the octahedra. The four other faces cannot be occupied by copper because too short distances to antimony would result. From the j.p.d.f. map and the 3D surface plots of the j.p.d.f. given in Fig. 8 the bottleneck character of the octahedra becomes obvious.

Conclusion

The crystal structures of the high-temperature and the low-temperature polymorph of Cu_3SbS_3 have been determined. The low-temperature modification γ-Cu_3SbS_3 is isotypic with Cu_3BiS_3, as already suggested by Whitfield [7]. A monoclinic low-temperature structure, cf. [6], could not be detected. In the high-temperature structure copper is disordered over at least five different sites. By a non-harmonic refinement of α-Cu_3SbS_3 a suggestion could be obtained for a diffusion pathway of copper atoms in the three-dimensional network of face sharing tetrahedra and octahedra of sulfur. Whereas copper is readily distributed over tetrahedral and trigonal-bipyramidal sites empty octahedra S_6 have been shown to be the bottlenecks for a three-dimensional movement of copper atoms. Due to experimental limitations concerning the highest possible measuring temperature the activation energy for copper diffusion in the high-temperature polymorph of Cu_3SbS_3 given in ref. [11] could not be verified but also not be rejected. For the proposed activation energy of ca. 270 meV a X-ray data collection at $T \geq 623$ K would have been necessary in order to obtain significant potentials of that height. In all modifications of Cu_3SbS_3 and also in Cu_3SbSe_3 short distances between the copper atoms are observed, but they are due to packing necessities rather than to d^{10}-d^{10} interactions. By contrast additional interactions between copper

and antimony seem to be present. This idea is supported by the existence of a threefold superstructure in sulfur rich compounds of the $Cu_3SbS_{3-x}Se_x$ series, where every third antimony is coordinated by a copper atom [26].

References

[1] Karup-Møller, S.; Makovicky, E.: Skinnerite, Cu_3SbS_3, a new sulfosalt from the Ilimaussaq alkaline intrusion, South Greenland. Am. Mineral. **59** (1974) 889–895.
[2] Nickel, E. H.; Nichols, M. C.: Mineral reference manual. Van Nostrand Reinhold, New York 1991.
[3] Dittrich, H.; Lux-Steiner, M.; Vaughan, D. J.; Lincot, D.; Boisivon, F.; Graeser, S.; Kunst, R.: New photovoltaic materials from systematic mineralogy. Proc. of the 12th European photovoltaic solar energy conference (1994) 587.
[4] Pfitzner, A.: Cu_3SbS_3: Zur Kristallstruktur und Polymorphie. Z. anorg. allg. Chem. **620** (1994) 1992–1997.
[5] Makovicky, E.; Balic-Zunic, T.: The crystal structure of skinnerite, $P2_1/c$-Cu_3SbS_3, from powder data. Can. Mineral. **33** (1995) 655–663.
[6] Makovicky, E.: Polymorphism in Cu_3SbS_3 and Cu_3BiS_3: The ordering schemes for copper atoms and electron microscope observations. N. Jb. Miner. Abh. **168** (1994) 185–212.
[7] Whitfield, H. J.: Polymorphism in skinnerite, Cu_3SbS_3. Solid State Comm. **33** (1980) 747–748.
[8] Matzat, E.: Die Kristallstruktur des Wittichenits, Cu_3BiS_3. Tschermaks Mineral. Petrogr. Mitt. **18** (1972) 312–316.
[9] Kocman, V.; Nuffield, E. W.: The crystal structure of wittichenite, Cu_3BiS_3. Acta Crystallogr. **B29** (1973) 2528–2536.
[10] Lugakov, N. F.; Movchanskyi, E. A.; Pokrovskyi, I. I.: Self-diffusion of copper and ionic-conductivity in Cu_3BiS_3. Vestsi Akad. Navuk B. SSR, Ser. Khim. Navuk **3** (1975) 42–44.
[11] Lugakov, N. F.; Lyashevich, A. S.; Movchanskii, E. A.; Pokrovskii, I. I.; Shimanovich, I. E.: Self-diffusion of copper in compounds of the copper(I) sulfide-antimony(III) sulfide system. Dokl. Akad. Nauk B. SSR **18** (1974) 825–827.

[12] Makovicky, E.; Skinner, B. J.: On crystallography and structures of copper-rich sulphosalts between 25–170 °C. Acta Crystallogr. **A31** (1975) S65.
[13] Makovicky, E: The phase transformations and thermal expansion of the solid electrolyte Cu_3BiS_3 between 25 and 300 °C. J. Solid State Chem. **49** (1983) 85–92.
[14] Pfitzner, A.: Cu_3SbSe_3: Synthese und Kristallstruktur. Z. anorg. allg. Chem. **621** (1995) 685–688.
[15] Petricek, V.: JANA96. Institute of Physics, Academy of Sciences of the Czech Republic, Prague, Czech Republic 1996.
[16] Rodriguez-Carvajal, J.: PROGRAM FULLPROF, unpublished. Version 3.1c, ILL 1996.
[17] Makovicky, E.; Skinner, B. J.: Studies of the sulfosalts of copper. VII. Crystal structures of the exsolution products $Cu_{12.3}Sb_4S_{13}$ and $Cu_{13.8}Sb_4S_{13}$ of unsubstituted synthetic tetrahedrite. Can. Mineral. **17** (1979) 619–634.
[18] Pfitzner, A.; Evain, M.; Petricek, V.: $Cu_{12}Sb_4S_{13}$: A temperature dependent structure investigation. Acta Crystallogr. **B53** (1997) 337–345.
[19] Kuhs, W. F.: Statistical description of multimodal atomic probability densities. Acta Crystallogr. **A39** (1983) 148–158.
[20] Hamilton, W. C.: Significance tests on the crystallographic R factor. Acta Crystallogr. **18** (1965) 502–510.
[21] Bachmann, R.; Schulz, H.: Anharmonic potentials and pseudo potentials in ordered and disordered crystals. Acta Crystallogr. **A40** (1984) 668–675.
[22] Hyde, B. G.; Andersson, S.: Inorganic crystal structures. Wiley, New York 1989.
[23] Pfitzner, A.: $(CuI)_2Cu_3SbS_3$: Copper iodide as solid solvent for thiometalate ions. Chem. Eur. J. **3** (1997) 2032–2038.
[24] Jerome, J. E.; Wood, P. T.; Pennington, W. T.; Kolis, J. W.: Synthesis of new low-dimensional quaternary compounds, KCu_2AsS_3 and KCu_4AsS_4, in supercritical amine solvent. Alkali metal derivatives of sulfosalts. Inorg. Chem. **33** (1994) 1733–1734.
[25] Kanatzidis, M. G.; Chou, J. H.: Isolation of β-Ag_3AsSe_3, $(Me_3NH)[Ag_3As_2Se_5]$, $K_5Ag_2As_3Se_9$, and $KAg_3As_2S_5$: Novel solid state silver thio- and selenoarsenates from solvento-thermal syntheses. J. Solid State Chem. **127** (1996) 186–201.
[26] Pfitzner, A.: Unpublished results.
[27] Bérar, J. F.; Lelann, P.: E.S.D.'s and estimated probable error obtained in Rietveld refinements with local correlations. J. Appl. Crystallogr. **24** (1991) 1–5.